Microfluid Nanofluid
DOI 10.1007/s10404-011-0830-5

RESEARCH PAPER

Thermo-pneumatic pumping in centrifugal microfluidic platforms

Kameel Abi-Samra · Liviu Clime · Ling Kong · Robert Gorkin III · Tae-Hyeong Kim · Yoon-Kyoung Cho · Marc Madou

Received: 23 March 2011 / Accepted: 30 May 2011

Abstract The pumping of fluids in microfluidic discs by centrifugal forces has several advantages, however, centrifugal pumping only permits unidirectional fluid flow, restricting the number of processing steps that can be integrated before fluids reach the edge of the disc. As a solution to this critical limitation, we present a novel pumping technique for the centrifugal microfluidic disc platform, termed the thermo-pneumatic pump (TPP), that enables fluids to be transferred the center of a rotating disc by the thermal expansion of air. The TPP is easy to fabricate as it is a structural feature with no moving components and thermal energy is delivered to the pump via peripheral infrared (IR) equipment, enabling pumping while the disc is in rotation. In this report, an analytical model for the operation of the TPP is presented and experimentally validated. We demonstrate that the experimental behavior of the pump agrees well with theory and that flow rates can be controlled by changing how well the pump absorbs IR energy. Overall, the TPP enables for fluids to be stored near the edge of the disc and transferred to the center on demand, offering significant advantages to the microfluidic disc platform in terms of the handling and storage of liquids.

Keywords Centrifugal · Microfluidic · Pumping · Valve · Thermal

K. Abi-Samra · L. Kong · R. Gorkin III · M. Madou (✉)
Department of Biomedical Engineering, University of California, Irvine, Irvine, CA 92697, USA
e-mail: mmadou@uci.edu

L. Clime
National Research Council-Industrial Materials Institute, Boucherville, QC J4B 6Y4, Canada

K. Abi-Samra · R. Gorkin III · T.-H. Kim · Y.-K. Cho · M. Madou
Ulsan National Institute of Science and Technology (UNIST), World Class University (WCU), Ulsan, South Korea

1 Introduction

With dimensions similar to standard compact discs (CDs), centrifugal microfluidic discs are automated, disposable, and portable diagnostic tools for point of care settings (Garcia-Cordero et al. 2010a; Haeberle et al. 2006; Lee et al. 2011; Madou et al. 2006; Steigert et al. 2006; Xi et al. 2010). Rotor-based microfluidic systems are plastic discs that have embedded micro-features, such as channels and chambers, designed to hold and manipulate small volumes of fluids. A defining feature of the microfluidic disc platform is that fluids are pumped by centrifugal forces generated by spinning the disc rather than using syringe pumps and fluidic interconnects. The field is quite established; rotor-based fluidic platforms emerged over 40 years ago and a handful of fluidic functions and biochemical applications have been demonstrated on these unique and promising tools (Gorkin et al. 2010a).

While manipulating fluids in microfluidic discs by centrifugal forces has several advantages, centrifugal pumping only permits fluids to travel uni-directionally; i.e., the force acts radially outwards creating a pressure on the liquid that forces it to move from the interior of the disc to the outer rim. As a consequence, all fluidic processes must occur along a limited path length, restricting the number of steps that can be integrated before fluids reach the edge. In order to overcome this critical limitation, microfluidic discs can be augmented through the introduction of additional

Published online: 17 June 2011

fluid manipulation methods, and hence additional forces, to free up more space and allow for more fluidic functions on a single disc.

To date, a handful of fluid handling techniques have been demonstrated that help to expand the working path length of fluidic conduits in microfluidic discs (Garcia-Cordero et al. 2010b; Gorkin et al. 2010b; Kong and Salin 2010; Noroozi et al. 2009; Siegrist et al. 2010b). Garcia-Cordero et al. (2010b) reciprocated fluids within the disc by capillary action generated from hydrophilic surfaces while Noorozi et al. (2009) used an *in-disc* compression chamber to reciprocate fluids by pneumatic energy. Also with an *in-disc* compression chamber, Gorkin et al. (2010b) demonstrated moving liquids short distances to the center. Overall, these techniques offer elegant approaches for expanding the working path but are limited in the movement they can provide for fluid transfer. Ideally, large solutions could be moved to the center of a rotating disc on command, enabling more efficient usage of space on the real-estate tight disc and the performance of lengthier assays. To meet this critical need, Kong and Salin used an external compressed air source to direct fluids to the center of a spinning disc (Kong and Salin 2010). However, the use of compressed air can be problematic as the injection of air can lead to contamination of embedded liquids and achieving steady streams of air can be challenging from compressed air sources.

To offer a novel fluid manipulation technique for the microfluidic disc platform that is easy-to-implement and integrate we present the thermo-pneumatic pump (TPP). Overall, in our approach, fluids are pumped toward the center of a rotating disc by the thermal expansion of air entrapped in the disc. The manipulation of fluids by thermally actuated mechanisms is quite well developed in the field of traditional, stationary, microfluidic platforms (Ha et al. 2009; Handique et al. 2001; Song and Lichtenberg 2005) but to the best of our knowledge has never been demonstrated on rotating microfluidic platforms. In our technique, fluids are only pumped out of a chamber when the generated pneumatic energy is larger than the opposing centrifugal force. As a fluid is pumped out a chamber and toward the center of the disc, more pressure, and therefore more heat applied to the pump, is needed to continue pumping due to the increasing volume of air in the emptying chamber. In comparison to previous approaches to move fluids toward the center (Garcia-Cordero et al. 2010b; Kong and Salin 2010), our approach does not require the integration of hydrophilic surfaces or the injection of compressed air. In addition, our TPP is the result of a structural design with no moving parts fabricated directly into the plastic of the microfluidic disc, facilitating its fabrication, and heat is delivered by peripheral infrared (IR) equipment, enabling the pumping of fluids toward the center while the disc is in rotation. As we will show, the TPP behaves in a predictable manner and flow rates from the pump can be controlled by changing how well the pump absorbs IR energy.

2 Materials and methods

2.1 Microfluidic disc fabrication

Microfluidic discs were designed using CAD software and fabricated using an assembly of 1 mm thick optically clear polycarbonate sheets (McMaster-Carr, USA) and 100 µm thick optically clear pressure sensitive adhesive (PSA) layers (DFM 200 clear 150 POLY H-9V-95, FLEXcon, USA). Features were milled into the polycarbonate sheets using a table top CNC (T-Tech, GA, USA-QuickCircuit 5000), and microchannels were cut into the 100-µm thick PSA layers using a cutter-plotter (Graphtec, Japan-Graphtec CE-2000). Further device fabrication details can be found in Siegrist et al. (2010b).

2.2 Microfluidic disc design

Two microfluidic designs were employed for experimentation: Design A (Fig. 1a) was created for the analytical evaluation of the pump's behavior, and Design B (Fig. 1b) was introduced to demonstrate the complete transfer of a fluid to a more centrally located reservoir. In both concepts, the microfluidic channel is oriented radially so that liquid moves in the opposite direction of the centrifugal forces when the disc is spinning. Design A serves as an implementation of the pump that facilitates analysis, as it is important to know the relationship between the distance travelled by the meniscus with respect to the applied thermal energy. In addition, the cross-sectional area of the microchannel in Design A is $\sim$0.35% of the cross-sectional area of the microfluidic reservoir, allowing us to consider the system to be equal to that of a large tank emptying by a small leak ("Pump characterization" section). As microfluidic discs are made of clear materials, 0.5 mm graduations printed on paper were placed below the device to allow for real-time measurement of the fluid levels in the microfluidic channel and reservoir.

Design B, in comparison to Design A, has a shorter microchannel length and is designed to manipulate a smaller volume of liquid (20 µl instead of 120 µl), both changes were necessary to reduce the transfer time of the fluid to the collection chamber. In addition, to encourage the complete emptying of the liquid from the microfluidic reservoir, a slight taper was given to help funnel liquid out of the chamber during the pumping process. It should be noted that in both microfluidic constructs (Designs A and

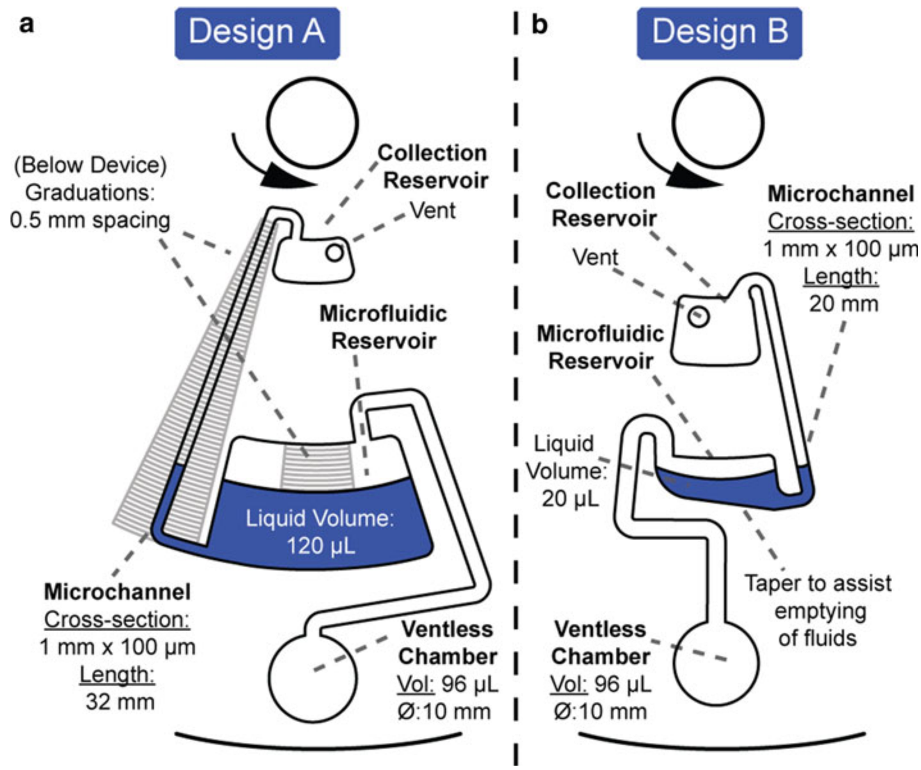

Fig. 1 **a** A design to assist the analytical evaluation. Graduations, printed on paper below the disc, allow for real-time measurement of liquid levels in the microchannel and microfluidic reservoir. **b** A design intended to be an implementation of the thermo-pneumatic pump that transfers a fluidic sample to a more central reservoir. *Note*: To simplify the illustration, loading holes are not shown on the microfluidic reservoirs

B), the ventless chamber was placed at the furthest distance possible from the microfluidic reservoir to reduce direct heating of the embedded liquid while still maintaining a 60-mm radius to the disc.

2.3 Experimental setup

Assembled microfluidic discs were mounted onto a specialized spin-stand that allowed for the programming of spin rates and the acquisition of one high-resolution image per rotation. Focused thermal energy was delivered to the rotating microfluidic disc in a non-contact manner via an IR heating platform consisting of a halogen lamp (12 V 75 W, International Technologies MA), an IR sensor (CSmicro, Optris, Berlin, Germany), a power supply, a data acquisition (DAQ) board, and a computer (Fig. 2). The halogen lamp was encased in a dichoric receptacle to focus the light onto the surface of the disc. Overall, the IR heating platform allows for the user to heat a $\sim$1-mm diameter spot on the surface of a rotating disc. The heating setup was calibrated using an IR thermal camera (Vario-CAM, Jenoptik, Germany) and thermal analysis software (Thermography Suite, IRcameras, Inc., MA). Temperatures obtained from the IR sensor were within 1°C of the temperature measurements taken by the IR thermal camera. Further details on the IR heating setup can be found in Abi-Samra et al. (2011).

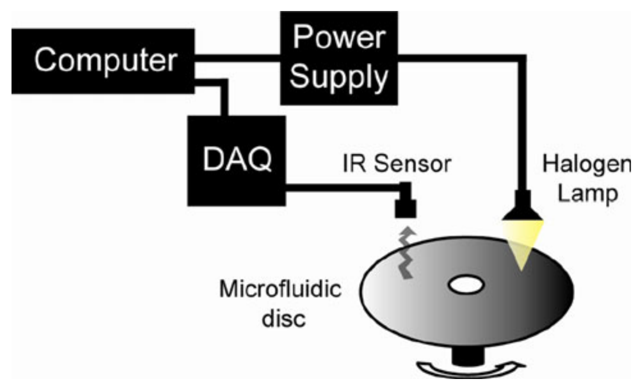

Fig. 2 Thermal energy is delivered to the rotating microfluidic disc by a setup consisting of a halogen lamp encased in a dichoric receptacle, an IR sensor, a power supply, a data acquisition board (DAQ), and a computer

2.4 Thermo-pneumatic pump characterization

The following experiments were performed to characterize the behavior of the pump in terms of the radial distance travelled by the evolving meniscus versus the applied thermal energy to the pump. First, 120 µl of colored water was introduced into the microfluidic reservoir of a disc containing Design A (Fig. 1a) followed by sealing the loading holes with single-sided adhesive (Fig. 3). It is important that the chamber is fully sealed so that pressure properly builds up in the microfluidic reservoir. Then, the IR lamp and IR sensor were aligned above the ventless

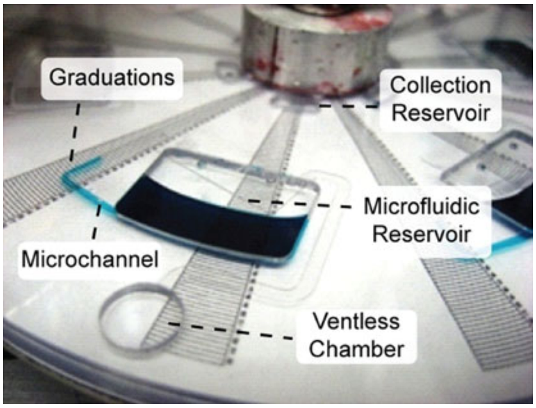

Fig. 3 Photograph of a microfluidic disc with an embedded thermo-pneumatic pump. Thermal energy is applied to the ventless chamber, positioned at the outer edge of the disc to minimize the direct heating of embedded liquids. Graduations of 0.5 mm, printed on paper below the device, facilitate real-time measurement of liquid levels

chamber of the microfluidic disc. Finally, spinning was commenced at a discrete rotational speed (600 or 1200 rpm). Before heat was applied to the ventless chamber, initial meniscus levels (R_0) were recorded for both the liquid in the microchannel and microfluidic reservoir. Then, with the IR heating platform, thermal energy was applied to the ventless chamber in 5°C increments starting from room temperature (~23°C) until the meniscus reached the collection reservoir. At each discrete temperature (i.e., each 5°C step), the radial position of the liquid in microchannel and microfluidic reservoir was recorded. All experiments were performed in triplicates.

2.5 Pump performance

The following experiments were performed to demonstrate the complete transfer of a fluidic sample to a more centrally located reservoir and to experiment with the pumping rates. First, 20 µl of colored water was loaded and sealed into a microfluidic disc featuring the TPP of Design B (Fig. 1b). Then, adequate heat was applied to the ventless chamber of the pump to transfer the fluid while spinning at 300 rpm (Fig. 4). Complete pumping of the 20-µl sample was achieved by applying 330 ± 1 K (57 ± 1°C) to the surface of the ventless chamber. Liquid was completely cleared from the microfluidic reservoir with assistance of the taper at the bottom edge of the reservoir as its shape helps to "funnel" out and continually collect the liquid outwardly as the disc spins.

As would be expected, the generated flow rates are a function of the material composition of the disc and the ability of those materials to absorb IR energy. For a configuration that had a low amount of IR absorption, a solid, 5-mm thick, optically clear polycarbonate disc was placed below a microfluidic disc featuring a pump of Design B (Fig. 1b). For a configuration that had a high amount of IR absorption, a solid, 5-mm thick, opaque black polycarbonate disc was placed below a microfluidic disc also featuring a pump of Design B (Fig. 1b). Experimentation for both configurations began after loading and sealing 20 µl of colored water into the disc. While spinning the disc at 300 rpm, adequate heat was applied to the ventless chamber to transfer all of the fluid from the microfluidic reservoir to the collection chamber. Flow rates in each configuration were measured by recording the total transfer

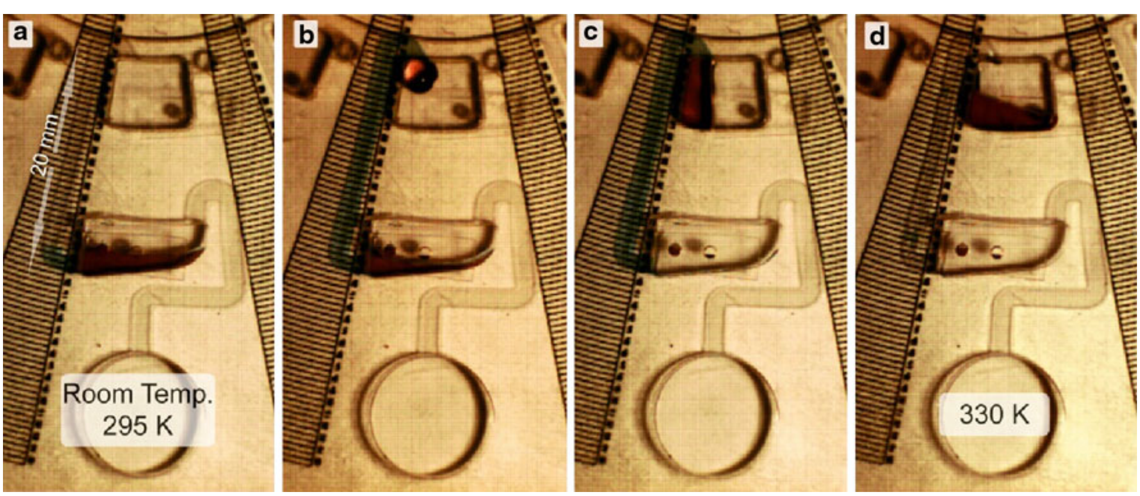

Fig. 4 Stroboscopic sequence of the transfer a 20-µl colored water sample by the thermo-pneumatic pump while the disc is rotating at 300 rpm. **a** Fluid resting at room temperature. **b**, **c** Filling of the collection chamber as heat is applied. **d** All fluid is transferred to the collection chamber after applying 330 ± 1 K to the surface of the ventless chamber

time for the 20-μl colored water sample. Trials were performed in triplicates.

3 Results and analysis

3.1 Pump characterization

Overall, the behavior of the TPP can be described in terms of the change in temperature on the surface of the pump, ΔT, and the radial position of the evolving meniscus of the fluid, ΔR, an analytical model for the operation of the pump is presented in this section.

The amount of air $V_c + V_a$ in the ventless chamber, microfluidic reservoir, and connecting channel (Fig. 5) is only locally heated by IR radiation, thus the distribution of temperature of the air will be non-uniform and result in having the largest values at the point where the IR energy is focused and the lowest values at the interface with the liquid. Naturally, this spatial variation of temperature brings a certain degree of difficulty in the analytical modeling. Therefore, in order to account for the non-uniform temperature gradient and to make the analytical treatment possible, a simplifying assumption is made—the air chamber is split in two regions where the temperature fields are considered uniform: one heated (V_h) and one unheated (V_R), such that $V_h + V_R = V_c + V_a$ is the total volume of the air. The separation between these two regions (V_h and V_R) is defined according to a fit parameter identified in the model from experimental data. In addition, if the cross-sectional area of the microfluidic reservoir is much larger than that of the microchannel, we can consider that the total volume of the air changes insignificantly as the liquid exits into the microchannel. In turn, we can safely consider that the total volume of the air in the ventless chamber, microfluidic reservoir, and connecting channel $V_h + V_R$, to be constant during the heating process; i.e., the heating of the air is an isochoric process (constant volume).

Before heat is applied to the pump, the distance of the liquid in the microchannel and microfluidic reservoir can be denoted by R_0, taken as the distance from the center of rotation (Fig. 5). This simplification holds if surface tension is neglected or if the contact angle is relatively close to 90° as it is for polycarbonate—the primary material of our microfluidic device (Siegrist et al. 2010a). Furthermore, we deal with large centrifugal forces, that is, large enough pressures to break the surface tension of the fluids in the system, and, again, this justifies this simplification.

It is also important to note that the relationship between the microfluidic reservoir and microfluidic channel can be approximated to be that of a large tank emptying by a small leak where the liquid level in the tank does not significantly change as a very small amount of fluid continually escapes. Once again, this approximation would require the cross-sectional area of the tank (the microfluidic reservoir) to be significantly larger than that of the leak (the microchannel). Thus, the liquid height in the microfluidic reservoir can be

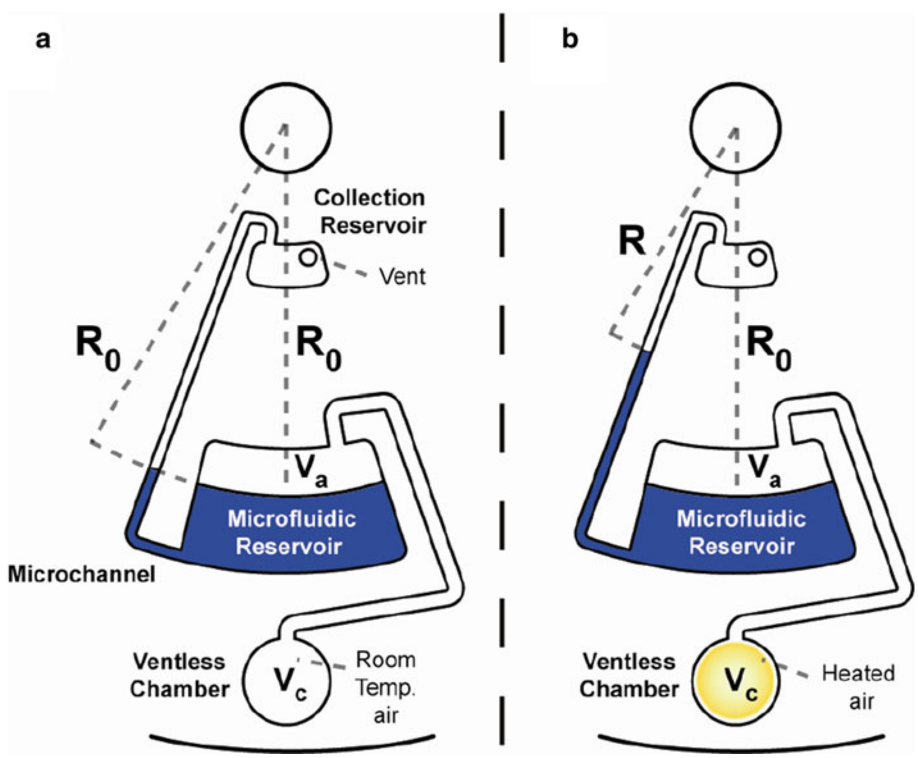

Fig. 5 Schematic showing the parameters used in the analytical evaluation of the thermo-pneumatic pump **a** before and **b** after heat is introduced to the ventless chamber. R_0 and R represent the distance of the liquid menisci with respect to the center of the disc. V_c and V_a represent the air volume in the ventless chamber and microfluidic reservoir, respectively

approximated to be constant, R_0, as fluid empties into the microfluidic channel (Fig. 5b). As a result of this approximation, the evolving meniscus in the microfluidic channel will be at $R < R_0$ from the center of rotation, when liquid level of the tank stays constant during the pumping process.

Thus, to develop an analytical model for the TPP's behavior, the assumptions made can be summarized as follows: (1) out of the total volume of air within the system, $V = V_h + V_R$, only the amount of V_h is heated by irradiation, (2) as the temperature in the heating chamber increases, the region of heated air, V_h, becomes larger (and V_R smaller), that is, V_h depends on the actual temperature of the system, and (3) the meniscus of the fluid in the microfluidic channel will be at $R < R_0$ from the center of rotation, when that of the tank stays at R_0 during the pumping process.

To understand how pressure is generated in the system, we must first look at the interaction between the ventless chamber and the microfluidic reservoir when thermal energy is applied to the pump. Based on the ideal gas law, before heat is introduced to the system, the following holds for V_h and V_R:

$$P_0 V_h = n_1 R_c T_0, \tag{1}$$

$$P_0 V_R = n_2 R_c T_0, \tag{2}$$

where P_0 is normal atmospheric pressure, n_1 and n_2 are the amount of substance (number of moles) of air in the regions V_h and V_R, respectively, R_c is the ideal gas constant and T_0 is the initial temperature of the ambient (unheated) air.

Once thermal energy enters the system through the ventless chamber, the temperature in the ventless chamber changes from T_0 to T, and the number of moles in the two regions changes accordingly. By considering again the ideal gas law for the two regions in the heated state, we get:

$$P V_h = n_1' R_c T \tag{3}$$

and

$$P V_R = n_2' R_c T_0. \tag{4}$$

Since

$$n_1 + n_2 = n_1' + n_2' \tag{5}$$

by substitution of Eqs. 1–4 into Eq. 5 we obtain:

$$\frac{P_0 V_h}{R_c T_0} + \frac{P_0 V_R}{R_c T_0} = \frac{P V_h}{R_c T} + \frac{P V_R}{R_c T_0} \tag{6}$$

and

$$P = P_0 \left(\frac{V_h + V_R}{V_h \frac{T_0}{T} + V_R} \right). \tag{7}$$

The change in pressure in the system can be written as:

$$\Delta P = P - P_0 = P_0 \left[\frac{V_h \left(1 - \frac{T_0}{T}\right)}{V_h \frac{T_0}{T} + V_R} \right]. \tag{8}$$

For convenience, we denote $b = V_h/(V_h + V_R) = V_h/V$ and $\Delta T = T - T_0$ and obtain:

$$\Delta P = \frac{P_0 b \Delta T}{T_0 + (1-b)\Delta T}. \tag{9}$$

A critical assumption, as previously stated, is that V_h increases as it is being heated. The physical basis of this assumption is that in our analytical treatment, the temperature corresponds to the experimental one, measured by the IR sensor at a certain point on the disc's surface. The measured temperatures by the IR sensor cannot fully account for the quantity of heat transferred from the IR lamp to the air trapped within the disc. Depending on the heating conditions, different gradients are possible, even when the same surface temperature is measured. Obviously, as the temperature in the system increases, the proportional volume of the heated air in the system, b, increases as well. A simple approximation of this assumption can be expressed mathematically as: $b = k\Delta T$, where k would be the rate of increase of b during the heating process. The heating will be more effective at large values of k, that is, when the heated region V_h increases faster and the temperature gradient becomes smaller. With the parameters b and k, both the temperature and temperature gradient are taken into consideration.

With b replaced by $k\Delta T$ in Eq. 9, we obtain:

$$\Delta P = \frac{P_0 k \Delta T^2}{T_0 + (1 - k\Delta T)\Delta T}. \tag{10}$$

Finally, the equation for the pressure generated in the system as a function of measured temperature is:

$$\Delta P = \frac{P_0 k \Delta T^2}{T_0 + \Delta T - k\Delta T^2}. \tag{11}$$

Now we must relate the generated pressure to the radial movement of the liquid in the disc. The hydrostatic equilibrium of the liquid in the system in the absence of any term related to surface tension can be written as:

$$\Delta P = P(R) - P_0 = \frac{1}{2}\rho\omega^2 (R_0^2 - R^2), \tag{12}$$

where ρ is the density of the liquid, ω is the fixed angular velocity, and R is the distance of the liquid meniscus to the center of the disc. We can express Eq. 12 in terms of the evolution of the liquid R^2/R_0^2 to give:

$$\frac{R^2}{R_0^2} = 1 - \frac{2}{\rho\omega^2 R_0^2}\Delta P. \tag{13}$$

Finally, replacing ΔP in Eq. 13 with Eq. 11 results in a formula that describes the behavior of the TPP in terms of the measured temperature, ΔT, required to move a liquid sample a certain radial distance, R, toward the origin:

$$\frac{R^2}{R_0^2} = 1 - \frac{2P_0}{\rho\omega^2 R_0^2}\frac{k\Delta T^2}{T_0 + \Delta T - k\Delta T^2}. \tag{14}$$

Since ρ and ω are constants, the two parameters left to be identified are R_0 and k. First, R_0 is easy to evaluate since it is the value of R, the distance of the liquid's meniscus to the center, at $\Delta T = 0$ (i.e., no heat is applied to the pump). As for k, we can easily make a link with ΔT_c, the change in temperature at which $R = 0$, the center of the disc.

Plugging in $R = 0$ and replacing $2P_0/\rho\omega^2 R_0^2$ with ε in Eq. 14, we obtain:

$$\Delta T_c = \frac{1 + \sqrt{1 + 4k(\varepsilon + 1)T_0}}{2k(\varepsilon + 1)}, \tag{15}$$

where

$$k = \frac{T_0 + \Delta T_c}{\Delta T_c^2(\varepsilon + 1)}. \tag{16}$$

Finally, Eq. 16 allows us to find the, once difficult to identify, parameter k, the model constant related to how efficiently the pump converts thermal energy to pneumatic pressure. The significance of this term (i.e., k) will be further described later.

Experimental and theoretical values for the radial movement of the liquid are presented in Fig. 6. Specifically, Fig. 6 is a plot of the normalized and squared distance of the evolving meniscus versus the change in applied temperature but can be considered to be a plot of ΔR versus ΔT. In the graph, the x-intercept indicates the ΔT_c for the pump at different RPMs. On the other hand, the y-intercept indicates the initial radial positions of the liquid in the microchannel, R_0. The experimental data (average with one confidence interval) agree with the predicted results (*solid lines*) generated from Eq. 14. Moreover, the small *error bars* demonstrate that the pump operates in a repeatable fashion.

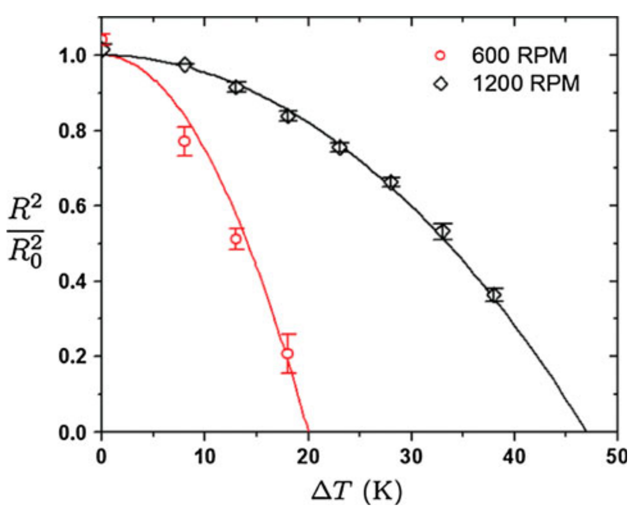

Fig. 6 Behavior of the thermo-pneumatic pump shown as a graph of the distance travelled by the meniscus versus the thermal energy applied. Experimental results are shown as discrete points with one standard deviation, whereas theoretical predictions are displayed as *solid color lines*. Pumping to the center of the disc was performed while spinning at 600 and 1200 rpm

As expected, the pump must work harder (i.e., requires a larger change in temperature for an equal amount of fluid pumped) when the disc is spinning at a higher rpm (1200 vs. 600 rpm) due to the existence of higher centrifugal forces. Thus, it could be assumed that the pump operates optimally when the disc is rotating at an angular velocity of zero (i.e., no rotation at all); however, this assumption is inaccurate. The pump functions in such a fashion that it requires the centrifugal force to continually push fluid outwardly in the microfluidic reservoir, providing a uniform vertical surface for pressurized air to act on. If the disc was stationary when heat is applied, liquid in the microfluidic reservoir would be disordered and pressurized air would pass either over or through the unorganized liquid, resulting in little or no pumping. Thus, the optimal rotational rate for the pump's operation would be the lowest RPM at which the surface tension of the fluid is broken.

3.2 Analysis of Pump performance

We can use the following analysis to quantify the performance of the pump in terms of how well thermal energy is converted to pneumatic energy. If we consider pumping liquid from R_0 to R_1 (where $R_1 < R_0$), the pressure required to perform this manipulation can be expressed as:

$$\begin{aligned}\Delta P &= P - P_0 - \frac{1}{2}\rho\omega^2\left(R_0^2 - R_1^2\right)\\ &= P_0\left(\left[\frac{T}{T_0}\right] - 1\right) - \frac{1}{2}\rho\omega^2\left(R_0^2 - R_1^2\right).\end{aligned} \tag{17}$$

The flow rate, Q, of the liquid in the channel is expressed as:

$$Q = \Delta P / R_{\mathrm{hyd}}, \tag{18}$$

where R_{hyd} is the hydrodynamic resistance of the channel and ΔP is the change in pressure required. The hydrodynamic resistance (R_{hyd}) of a rectangular channel, length (L) and rectangular cross-section (w by h where $h < w$), and a fluid of viscosity η can be approximated by:

$$R_{\mathrm{hyd}} \approx \frac{12\eta L}{1 - 0.63\frac{h}{w}}\frac{1}{h^3 w}. \tag{19}$$

However, as the amount of thermal energy needed to move a fluidic sample increases as the fluid leaves its initial reservoir, we need to express ΔP over the total range in temperature, which is done by integrating Eq. 11 from $\Delta T_{\min}$ to $\Delta T_{\max}$:

$$\Delta P_{\mathrm{avg}} = \frac{1}{\Delta T_{\max} - \Delta T_{\min}} \int_{\Delta T_{\min}}^{\Delta T_{\max}} \frac{P_0 k \zeta^2}{T_0 + \zeta - k\zeta^2} \mathrm{d}\zeta, \quad (20)$$

where $\Delta T_{\min}$ is the change in temperature required to initially move the fluid through the channel, $\Delta T_{\max}$ is the change in temperature required to completely transfer the fluid to its final location and $\zeta = \Delta T$ is an integration variable. Using ΔP_{avg} in Eq. 18 instead of ΔP in Eq. 17, we are able to get an average flow rate for the pump and estimate the time needed to transfer a certain amount of liquid. Moreover, Eq. 20 allows us to link the average flow rate to a given configuration of the pump by the means of the constant k.

Once again, the model parameter k is related to how quickly the TPP absorbs heat and generates pneumatic energy. A pump with a large k constant would indicate quicker heating of the entrapped air and faster generation of pneumatic pressure, in comparison to a pump that has a smaller k value. Ultimately, k is a result of the materials that are incorporated into the pump device and how quickly those materials absorb and distribute IR energy and heat the entrapped air.

As described in the "Pump performance" section, a low-IR absorption and high-IR absorption configuration for TPPs were employed to experimentally determine the generated flow rates and resulting k constants, Table 1. As expected, the high-IR absorption configuration resulted in larger generated flow rates than the low-IR absorption configuration. In fact, the resulting flow rate from the high-IR absorption configuration is about twice as large. From the analysis, we know that as the generated flow rate from a pump increases, so does the pump's associated model constant k. Experimentally this trend was observed and the k constant for the high-IR absorption configuration was larger than the low-IR absorption configuration. Thus, we have a preliminary demonstration of pumping rate control by changing the materials around the pump; however, options do exist to use a wide range of materials to give a broad spectrum of predictable and repeatable flow rates from the TPP.

Table 1 Flow rates generated and calculated model constant k (the model constant related to how fast the thermo-pneumatic pump absorbs IR energy and heats the entrapped air) associated with each configuration

Configuration	Rotational speed (rpm)	Flow rate (μl/min)	Calculated model constant k ($\times 10^{-4}$ deg^{-1})
Low IR absorption			
Top	300	8.26 ± 0.46	3.73 ± 0.78
Microfluidic disc with Thermo-pneumatic pump			
Bottom			
Optically clear polycarbonate disc (5 mm thick)			
High IR absorption			
Top	300	17.6 ± 1.5	5.74 ± 0.91
Microfluidic disc with Thermo-pneumatic pump			
Bottom			
Opaque black polycarbonate disc (5 mm thick)			

4 Discussion

The TPP is an easy-to-implement technique for the precise manipulation of fluids in centrifugal microfluidic discs. Fluids are mobilized by the TPP only when sufficient pneumatic energy has been generated to counter the centrifugal force holding the fluids back. Such control of fluids in microfluidic discs is critical in the development of micro total analysis systems (μTAS). For example, through the actuation of wax valves by a mobile laser system, Cho et al. (2007) were able to achieve the multiple valving steps necessary to perform DNA extraction from whole blood. The wax plugs, which acted as physical gating mechanisms, were critical to the assay processing, as the high speeds required for plasma separation from whole blood would have broken any passive valving schemes presented to date in the literature (viz., hydrophobic, hydrophilic, siphon, and Coriolis) (Ducrée et al. 2007; Kim et al. 2008; Madou et al. 2006; Siegrist et al. 2010b). We envision the TPP as an alternative technique to using wax plugs or other active valving techniques (Garcia-Cordero et al. 2010c; Abi-Samra et al. 2011) for the controlled release of fluids due its simplicity. Based on the thermal expansion of air, the TPP has no moving components making it straightforward to fabricate in monolithic devices, while active valves pose significant roadblocks in fabrication due to the need to embed physical gating mechanisms.

A significant advantage of the TPP is that it does not require hydrophilic surfaces, thus it can be made using a wide range of materials, including many polymers that are natively hydrophobic. As its pumping mechanism is based on the interplay of pneumatic energy and centrifugal forces, the pump behaves predictably and can be straightforwardly modeled which further facilitates its implementation in future devices. In addition, the generated pumping rates can be simply controlled by changing how well the disc device absorbs IR energy. In our setup, the highest pumping rate achieved was 17.6 ± 1.5 µl/min; however, further study is warranted into exploring the boundaries of generated pumping rates. Outside of the disc, a simple peripheral IR heating platform is required to actuate the pump, adding no complexity to the disposable disc. Other modes of heating beyond the employed IR heating setup (e.g., forced convection, thermoelectrics, or laser diodes) could potentially be adapted for the actuation of the pump. In our strategy, fluids are pushed to the center of a rotating disc by air entrapped in the disc device rather than air that is introduced from an external compressed air source (Kong and Salin 2010), reducing the risk of contamination. As a result of storing downstream fluids near the edge and transferring them to the center as needed, the TPP can uniquely be used to more efficiently use space on the real-estate-limited disc. Large solutions can be stored near the outer edge of the disc and moved centrally when needed, freeing up space for the storage of other liquids. It should be noted that for simplicity the ventless chamber of the pump was designed in a circular shape; however, the ventless chamber can take form as an arch-shaped chamber that "bends" around the radius of the disc, further freeing up space.

As the mechanism for pumping is ultimately dependent on heating a region of the disc, the risk of heating embedded liquids above room temperature is a valid concern. To avoid the direct heating of liquids, the region to be heated, termed the ventless chamber (Fig. 1), was placed at the furthest possible distance from the fluids to be pumped while still maintaining a 60-mm radius to the disc. In the demonstrations, the surface of the ventless chamber was heated to 57 ± 1°C to transfer a 20-µl sample to a more centrally located reservoir. It should be noted that the temperature of the embedded liquids was not directly monitored due to the difficulties in accurate measurement of a system in rotation and further study into examining the transfer of heat from the entrapped air to the liquids is warranted. Nevertheless, several parameters of the system (e.g., rotational frequency of the disc, volume of liquid to be transferred, hydraulic resistance of conduits) can be optimized to lower the final temperature required to pump a liquid. In addition, the final disc device can be coated with IR absorbing or reflecting materials to optimize heat distribution. However, heat is an essential part of many biochemical protocols (e.g., PCR) and the heating of embedded liquids above room temperature may not be a concern, rather, an advantage. It is envisioned that the TPP can be used in conjunction with a growing number of heat-based processes for microfluidic devices (e.g., valving, reagent storage and release, sample incubation, and thermocycling). Therefore, the TPP adds to the toolbox of capabilities for the microfluidic disc platform without requiring equipment beyond a peripheral thermal management system.

5 Conclusions

The centrifugal microfluidic disc is largely a uni-directional platform that supports a limited number of processing steps before fluids reach the edge of the disc. To address this critical issue, we present a novel pumping technique, termed the TPP, based on the thermal expansion of air to move fluids from the edge to the center of a rotating disc. In comparison to other techniques geared to improve the real-estate on the microfluidic disc platform, our approach does not require hydrophilic surfaces or the injection of compressed air, enabling a wide choice of materials for fabrication and promoting the integrity of the device. Furthermore, the pump can be easily made in monolithic devices as it has no moving parts. The TPP behaves predictably as it is essentially based on the interplay of pneumatic energy and centrifugal forces and can be straightforwardly modeled, facilitating its realization in future devices. In addition, the generated pump rates can be easily controlled by changing how well the device absorbs IR energy. Another key benefit is that the TPP adds to the growing number of heat-based mechanisms for microfluidic devices (e.g., valving) and, in turn, promotes the simplification and unification of the peripheral equipment. Overall, the thermo-pneumatic offers significant advantages to the microfluidic disc platform in terms of the handling and storage of liquids and enables microfluidic discs that can perform lengthier biochemical assays.

Acknowledgments The authors wish to thank the WCU (World Class University) program (R32-2008-000-20054-0) and Genome Québec for funding of the presented research.

References

Abi-Samra K, Hanson R, Madou M, Gorkin RA III (2011) Infrared controlled waxes for liquid handling and storage on a CD-microfluidic platform. Lab Chip 11(4):723–726. doi:10.1039/c0lc00160k

Cho YK, Lee JG, Park JM, Lee BS, Lee Y, Ko C (2007) One-step pathogen specific DNA extraction from whole blood on a centrifugal microfluidic device. Lab Chip 7(5):565–573. doi:10.1039/B616115D

Ducrée J, Haeberle S, Lutz S, Pausch S, Stetten FV, Zengerle R (2007) The centrifugal microfluidic Bio-Disk platform. J Micromech Microeng 17(7):S103–S115. doi:10.1088/0960-1317/17/7/S07

Garcia-Cordero JL, Barrett LM, Kennedy RO, Ricco AJ (2010a) Microfluidic sedimentation cytometer for milk quality and bovine mastitis monitoring. Biomed Microdevices 12(6):1051–1059. doi:10.1007/s10544-010-9459-5

Garcia-Cordero JL, Basabe-Desmonts L, Ducrée J, Ricco AJ (2010b) Liquid recirculation in microfluidic channels by the interplay of capillary and centrifugal forces. Microfluid Nanofluid 9(4): 695–703. doi:10.1007/s10404-010-0585-4

Garcia-Cordero JL, Kurzbuch D, Benito-Lopez F, Diamond D, Lee LP, Ricco AJ (2010c) Optically addressable single-use microfluidic valves by laser printer lithography. Lab Chip 10(20): 2680–2687. doi:10.1039/c004980h

Gorkin R, Park J, Siegrist J, Amasia M, Lee S, Park JM, Kim J, Kim H, Madou M, Cho YK (2010a) Centrifugal microfluidics for biomedical applications. Lab Chip 10(14):1758–1773. doi:10.1039/b924109d

Gorkin R, Clime L, Madou M, Kido H (2010b) Pneumatic pumping in centrifugal microfluidic platforms. Microfluid Nanofluid 9(2): 541–549. doi:10.1007/s10404-010-0571-x

Ha SM, Cho W, Ahn Y (2009) Disposable thermo-pneumatic micropump for bio lab-on-a-chip application. Microelectron Eng 86(4–6):1337–1339. doi:10.1016/j.mee.2008.12.046

Haeberle S, Brenner T, Zengerle R, Ducrée J (2006) Centrifugal extraction of plasma from whole blood on a rotating disk. Lab Chip 6(6):776–781. doi:10.1039/b604145k

Handique K, Burke DT, Mastrangelo CH, Burns MA (2001) On-chip thermopneumatic pressure for discrete drop pumping. Anal Chem 73(8):1831–1838

Kim J, Kido H, Rangel RH, Madou M (2008) Passive flow switching valves on a centrifugal microfluidic platform. Sens Actuators B 128(2):613–621. doi:10.1016/j.snb.2007.07.079

Kong MCR, Salin ED (2010) Pneumatically pumping fluids radially inward on centrifugal microfluidic platforms in motion. Anal Chem 82(19):8039–8041. doi:10.1021/ac102071b

Lee BS, Lee YU, Kim HS, Kim TH, Park J, Lee JG, Kim J, Kim H, Lee WG, Cho YK (2011) Fully integrated lab-on-a-disc for simultaneous analysis of biochemistry and immunoassay from whole blood. Lab Chip 11(1):70–78. doi:10.1039/c0lc00205d

Madou M, Zoval J, Jia G, Kido H, Kim J, Kim N (2006) Lab on a CD. Annu Rev Biomed Eng 8(1):601–628. doi:10.1146/annurev.bioeng.8.061505.095758

Noroozi Z, Kido H, Micic M, Pan H, Bartolome C, Princevac M, Zoval J, Madou M (2009) Reciprocating flow-based centrifugal microfluidics mixer. Rev Sci Instrum 80(7):075102. doi:10.1063/1.3169508

Siegrist J, Amasia M, Singh N, Banerjee D, Madou M (2010a) Numerical modeling and experimental validation of uniform microchamber filling in centrifugal microfluidics. Lab Chip 10(7):876–886. doi:10.1039/b917880e

Siegrist J, Gorkin R, Clime L, Roy E, Peytavi R, Kido H, Bergeron M, Veres T, Madou M (2010b) Serial siphon valving for centrifugal microfluidic platforms. Microfluid Nanofluid 9(1):55–63. doi:10.1007/s10404-009-0523-5

Song WH, Lichtenberg J (2005) Thermo-pneumatic, single-stroke micropump. J Micromech Microeng 15(8):1425–1432. doi:10.1088/0960-1317/15/8/007

Steigert J, Grumann M, Brenner T, Riegger L, Harter J, Zengerle R, Ducrée J (2006) Fully integrated whole blood testing by real-time absorption measurement on a centrifugal platform. Lab Chip 6(8):1040–1044. doi:10.1039/b607051p

Xi Y, Duford DA, Salin ED (2010) Automated liquid-solid extraction of pyrene from soil on centrifugal microfluidic devices. Talanta 82(3):1072–1076. doi:10.1016/j.talanta.2010.06.007